*Association of Metallurgical Engineers of Serbia* *Scientific paper*
*AMES* *UDC: 669.14.018.8:667.637.27;667.637.27*

# SOL–GEL BIOACTIVE GLASS COATING FOR IMPROVEMENT OF BIOCOMPATIBLE HUMAN BODY IMPLANT

Mehdi Mazar Atabaki[1,2*], Rabi'atuladawiyah Jafar[1], Jamaliah Idris[1]

[1]*Department of Materials Engineering, Faculty of Mechanical Engineering, University Technology Malaysia, Skudai, Johor Bahru, Malaysia 81310*
[2]*Institute for Materials Research, the School of Process, Environmental and Materials Engineering, Faculty of Engineering, University of Leeds, Leeds, UK*

*Received 24.05.2010*
*Accepted 01.09.2010*

## Abstract

Stainless steel 316L is widely used for implantation purposes in orthopedic surgery due to its corrosion resistance, mechanical properties and absolutely low cost. In this study, in order to increase the life span of the implantation, coating process is applied on the stainless steel implant to form a thin film barrier. The hydroxyapatite (HA) coating is used to protect the surface of the implant material. Dip Sol-gel method is applied to produce HA coating on stainless steel due to its low cost and easy to produce. This technique provides several advantages in the control of microstructure and the thickness of the coatings. HA is prepared with different amount of chemical additives, $P_2O_5$, $Na_2C0_3$, and $KH_2PO_4$, in order to obtain better gel. The protective atmosphere during sintering process accomplished after sol-gel coating produces good uniformity of coating material and significantly a large reduction in the porosity of the coating film. The coated specimens have been characterized by using scanning electron microscopy (SEM), X-ray diffraction analysis (XRD) and Fourier transform infrared spectroscopy (FT-IR). Observations showed that the coating film is uniform at 900 °C of sintering temperature in vacuum atmosphere. In addition, mechanical properties of the films, such as tensile strength and hardness are studied. The highest value of tensile test and hardness is obtained at 900 °C of sintering temperature. The coatings are dense and tightly attached to the underlying substrates, reaching an average strength of 45.9 MPa.

*Key words: Dip coating; Sol-gel; Implant material; Sintering; Strength; Hardness*

* Corresponding author: Mehdi Mazar Atabaki, m.mazaratabaki@gmail.com

## Introduction

Stainless steel 316L (ASTM F138) is being widely used for implantation purposes in orthopedic surgery due to its corrosion resistance, mechanical properties and absolutely low cost [1]. In order to increase the life span of the implantation, coating process is widely applied on the stainless steel implant to form a thin film to protect the implant from corrosive environments [2]. Currently, the hydroxyapatite (HA) coating is the most common technique used to protect the surface of the implant material [3].

Unfortunately, the mechanical strength of hydroxyapatite is fairly poor and therefore, for many purposes, bulk materials cannot be used as implants. In order to obtain bioactive materials with high mechanical strength, usually metal implants are coated with a thin layer of hydroxyapatite [4]. The main problem associated with this technique is the lack of an exact stoichiometry and the occurrence of glassy phases in the ceramic layer. Some of these additional phases do not show a bioactive behavior or are dissolved in the biological environment [5].

Compared with the melting methods, the sol-gel processes have the advantage of low reaction temperature and homogenous composition in particles. Some sol-gel bioactive glasses in the system of $SiO_2$-CaO-$P_2O_5$ have been widely studied [6, 7]. It has been shown that when a hard tissue is coated with artificial biomaterial such as HA good mechanical performances and excellent biocompatibility may be expected [8]. HA, with the formula of $Ca_{10}$ $(PO_4)_6(OH)$ $_2$, is also used as coating material in plastic and orthopedic surgery. Moreover, HA is the similar mineral component of bone and it has been shown to encourage bone growth when implanted in the body. It also does not invoke an immune reaction [9].

Nevertheless, it is possible to replace some inorganic components for organic ones in order to obtain higher plasticity [10]. The combination of the sol–gel organic–inorganic (hybrid) films with the addition of bioactive particles from the system $SiO_2$–$P_2O_5$–CaO has shown a good adherence of the cement-less implants with the pre-existing bone [11]. Various types of sol gel coating can be applied as substrate coatings. For instance, dip coating, spray coating, flow coating, spin coating, and particulate coating are the most popular techniques. However, dip coating is the most effective coating method for 316L stainless steel substrates [12].

In view of the above, an attempt has been made to replace a new composition of sol-gel bioactive glass with different percentage of components through dip coating method. Another aim of this work was to obtain a homogenous sol-gel coatings containing bioactive glass, glass ceramic and HA particles on stainless steel 316L by sintering process in argon and vacuum atmospheres using various time and temperature. It was found that the sol–gel HA coatings strongly attach to the 316L substrates at sintering temperature of 900°C in a vacuum atmosphere.

## Materials and Method

*Substrates Preparation*

Stainless steel 316L plates with the composition, (chemical composition in this paper is given in wt %) C 0.025, Mn 2.05, Si 1, P 0.045, S 0.03, Ni 13.5, Cr 17.4, and Mo 3, cut to 10mm width, 15mm length, and 2mm thickness were used as substrates. The surfaces of specimens were grinded and polished to remove the roughness. After

that specimens were washed with detergent, and then passivated in nitric acid in order to maximizing the essential corrosion resistance of stainless steels. During nitric acid passivation, specimens were soaked in acid nitric (20%) for 30 minutes and then were rinsed with water, following by drying in air. Next, specimens were ultrasonically cleaned by immersing in acetone in an ultrasonic bath.

*Sol-Gel Preparation*

Sol-gel was produced depending on the chemical reaction between the sol solution and the chemical additives. Better gel was prepared based on the weight percentage of the chemical additives and time of ultrasonic treatment.

In this investigation sol-gel coating process was carefully controlled by the immersing time for varying coating thickness. The glass coating material was prepared based on HA with adding $P_2O_5$, $Na_2C0_3$, and $KH_2PO_4$ additives to obtain the better gel. In terms of viscosity of solution, different percentages of composition were examined to finally achieve the best viscose glass coating material. In order to obtain the sol, calcium phosphate or hydroxyapatite (HA) was mixed with fixed amount of ethanol in a sealed container under dynamic stirring for 24 hours. By using magnetic stirrer, the mixture of ethanol and HA (Aldrich, USA) were continuously agitated and stirred at 350 rpm for 24 hours. Then, the sol was leaved for a few hours to make it stable. The fine and homogeneous sol-gel was obtained by adding some biocompatible ceramic ($P_2O_5$, $Na_2CO_3$, and $KH_2PO_4$) into the stable sol. The colloidal sol was blended with homogenizers chemical using ultrasonic treatment (Vibra Cell Sonic) to obtain the gel.

In the first trial, the amount of HA was less than 25 wt% and chemical additives had the composition 40 $P_2O_5$, 4 $KH_2PO_4$, 4 $Na_2CO_3$, and a drop of glycerol. The result for the first trial in obtaining sol-gel showed small viscousity in final gelatin, while the second trial solution showed a good viscous final gelatin. In the second trial, the percentage of HA was 25 and chemical additives had the composition 43 $P_2O_5$, 4 $KH_2PO_4$, 18 $Na_2CO_3$, and 4 drops of glycerol. As a result, the sol solution turned into superior viscous gel.

$P_2O_5$ additive was added to the HA with the purpose of providing a good adherence of the sol-gel coating to the substrates. However, mechanical properties of commercial HA can be significantly improved by adding $P_2O_5$ and $Na_2CO_3$ without altering its biocompatibility [12]. $KH_2PO_4$ and glycerol were added to the HA solution in order to reduce the precipitation between the coating material and the stainless steel substrates during sintering process at high temperature. In addition, these additives also improved the gelatin of sol-gel coating with a small amount of released hydrogen.

All specimens were dipped into the sol-gel and then they were held at room temperature for 7 hours. The dipped specimens were then dried in air for 24 hours. Prior to sintering, the dip coating specimens were completely dried.

*Ultrasonic Treatment*

The Vibra-Cell ultrasonic treatment was performed to homogenize the sol-gel. In addition, portable probe was used for preparation, dispersion, cleaning, and desegregation of sol solution. During the ultrasonic process, the chemical additives were added to the sol solution to get better gelatin.

*Sintering*

In this work argon and vacuum furnace were used in order to sinter the coating layer on the stainless steel substrates. This process reduces dehydroxylation of the coating material. For this purpose coated specimens were sintered in argon and vacuum furnace with an annealing temperature below the melting point of HA. In this research, various sintering temperatures were applied to obtain good mechanical properties for biocoating. It should be pointed out that the dip coated substrates were sintered at 300, 600, and 900°C for 15, 30 and 60 min under argon and vacuum atmospheres.

*Characterization*

Scanning electron microscopy (SEM) and energy dispersive X-ray analysis (EDX) techniques were performed by Phillips XL 30 to study the microstructure and morphology of the biocoating coatings. EDX analysis was utilized to estimate the composition of the coatings.

X-ray diffraction analysis (XRD) was used by a Philips X'Pert-MPD system with a Cu Kα wavelength of 1.5418 $A^{\circ}$ to analyze the crystal structure and phase present in the prepared biocoating. The diffractometer was operated at 40 kV and 30mA at a $2\theta$ range of 20–70$^{\circ}$ employing a step size of 0.02$^{\circ}$/s.

The formation of the apatite layer was analyzed using Fourier transform infrared spectroscopy (FT-IR) (Bomem, MB-100) in the range of 4000–100 $cm^{-1}$.

The pore diameter distribution was calculated by the Barrett- Joyner-Halenda method applied to the desorption curves. Larger pore size distributions were determined by intrusion mercury porosimetry (Poresizer 9320, Micromeritics, USA).

*Mechanical Properties of Biocoating*

The pull-out test was performed at a crosshead speed of 1 mm/min, using universal mechanical testing machine (Instron). Average of at least three test specimens was used for each experimental point.

The Vickers (HV) hardness test is also used to determine the value of biocoating hardness. The Vickers test had two different force ranges, micro and macrohardness. The load range for microhardness was 10 to 1000 g, while the macro was 1 to 100 kg. Indent time of 20 s was applied.

## Results and Discussion

*Study of the Microstructure and Morphology of the Biocoatings*

Homogeneous and crack-free coatings were obtained on biocompatible 316L stainless steel implant at higher sintering temperatures. The average thickness measured for the coating film without and with small and big particles are almost 2.2, 5.4 and 4.3 mm, respectively. However, the biocoating on 316L stainless steel has a critical thickness (>5 μm), defined as the greatest thickness without cracks [13].

Low-temperature formation and fusion of the apatite crystals have been the main contributions of the sol–gel process, in comparison with conventional methods. Temperatures higher than 1000 °C are usually required to sinter the fine apatite crystals prepared by wet precipitation method, whilst several hundred degree Celsius lower than

above are needed to densify sol–gel HA. Also, sol–gel process for HA preparing usually can produce fine-grain microstructure containing a mixture of submicron crystals. These crystals can be better accepted by the host tissue.

The surface morphology of the HA coating subjected to sintering temperatures at 300, 600 and 900 ºC on stainless steel substrates is shown in Figs. 1(a)-(d), respectively. The porosity of specimens sintered at 300 ºC is much higher than those of sintered at 600 and 900 ºC. The big pores on the coated surface which were related to specimens sintered at 300ºC lead to the initial cracks on the surface into the interior of the coating layer. The good uniformity of HA coated substrate in terms of composition and low pores is obtained as the sintering temperature increases. After sintering at 600 and 900 ºC, the pore size decreases due to a uniform film. The pore sizes at 900 ºC are in average less than 1.5µm as shown in Fig. 1 (c). The pores with sizes from 0.5 to 1µm are connected to form a continuous network, which may be of advantage for the circulation of physiological fluid throughout the coating when it is used for biomedical purposes [13]. It is also important to take into account the sintering time. As shown in Fig. 1 (d), even though the porosity is smaller the surface of coating film is not uniform enough due to the shorter sintering time. Therefore, the sintering time must be regarded as an important parameter affecting the microstructure of surface coating.

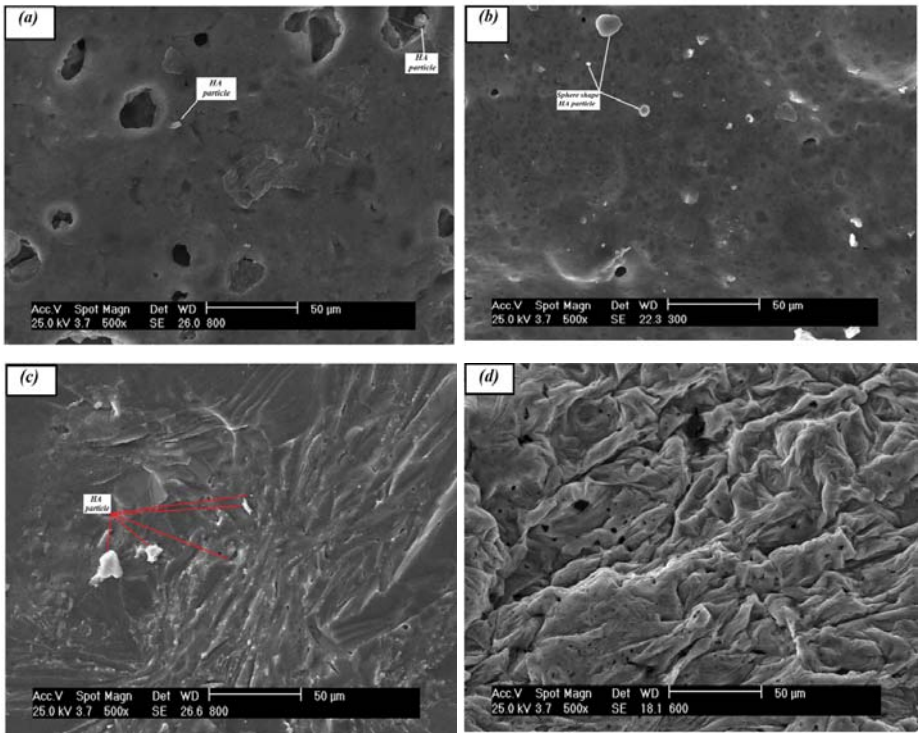


*Fig.1. Microstructure of HA surface coating on stainless steel substrates. (a) sintered at 300 ºC for 60 min; (b) sintered at 600 ºC for 60 min; (c) sintered at 900 ºC for 60 min; (d) sintered at 900 ºC for 15 min.*

There is a substantial volume contraction and internal stress accumulation due to the large amount of evaporation of solvents and water in this technique. Cracks were easy to form due to this internal stress if the film formation conditions were not carefully controlled. In fact, in some cases in spite of using heat treatment for sol–gel coatings, the cracks stemmed substantially from internal stress accumulation. Although the coatings appear relatively dense, very small surface microcracks (0.01 wide and 0.5 mm long) are visible in the 300 °C specimens.

The deposition of semicrystalline HA is considered as a first signal of bioactivity [14]. As the coatings containing particles present a high reactive area, it is not unexpected that they are able to induce a higher proportion of a HA deposition on the surface. Nonetheless, it is important to consider another aspect related to these coatings that is the protective function. It has been studied that the particle reaction to form a HA breaks the coating that contains the particles inducing cracks in the surrounding of the particle [14]. This fact could result in local corrosion of the substrate if the flaws reach the substrate.

Thermal treatment of HA sol-gel films under vacuum environment was chosen to avoid metal oxidation. However, this leads to small structural instability of the HA coating (i.e. evolution of structural water under vacuum environment) during thermal treatment. Therefore, thermal treatment temperature was selected at a minimum level which assured sufficient quality of HA film, in terms of crystallinity, film integrity, and adhesion to the substrate.

It should be noted that the synthesis of HA requires a correct molar ratio of 1.67 between Ca and P in the final product. A number of combinations between Ca and P precursors were employed for sol-gel HA synthesis. Bearing in mind the difference in chemical activity of the precursors, such as hydrolysis, polycondensation, etc., it appears that the temperature required to form the apatitic structure mainly depends on the chemical nature of the precursors. Gross et al. [15] used calcium diethoxide ($Ca(OEt)_2$) and triethyl phosphate ($PO(OEt)_3$) to form a pure HA phase at temperatures above 600°C. They also found that ageing time longer than 24 h is critical for the solution system to stabilize a produced single phase HA [16]. In one of previous papers [17] a gel route was developed using calcium nitrate and phosphonoacetic acid ($HOOCCH_2PO(OH)_2$) in an aqueous solution and obtained a pure HA powder at 700°C. The crystallinity of HA improved with temperature up to 1100 °C. Qiu et al. [18] used calcium nitrate and ammonium dihydrogen phosphate ($NH_4H_2PO_4$) to synthesize HA in a highly basic solution. They obtained HA at calcinations temperatures of 400-1100 °C and indicated that the crystallinity of the HA was improved with increasing temperature.

By closely examining Figs.1, it can be observed that some initial sintering occurred between the HA crystals (white halos). On the sol-gel surface some well-sintered sections can also be observed, which are believed to be due to smaller HA crystallites providing better sinterability at higher temperatures. The pores developed in the coating are believed to be a result of evolution of gas during thermal pyrolysis of residues. In specimens with higher amount of pores, especially those sintered at low temperature, there is potential risk to form cracks in the coatings from the HA sols because of relatively large amount of organic residues.

*FT-IR Examination*

The two triply degenerate IR active modes situated in the region of 800–900 $cm^{-1}$ are due to the presence of P–O stretching vibrations. These peaks are present in all the coatings and the two triply degenerate modes were distinguishable. Fig. 2 shows the FT-IR spectra of the coatings at different sintering temperatures. For specimens sintered at 300 °C, one relatively broad band at 300–400 $cm^{-1}$ and a small one at 800–850 $cm^{-1}$ were observed, which can be attributed to the absorption modes associated with $PO_4$ groups. It is believed that there are four vibrational modes present for phosphate ion $\nu_1$, $\nu_2$, $\nu_3$ and $\nu_4$ all the four modes are IR active and are observed for all the spectra of HA [19].

The $\nu_1$ and $\nu_3$ phosphate bands in the region of 800–900 $cm^{-1}$ and $\nu_4$ absorption bands in the region of 200–500 $cm^{-1}$ are used to characterize apatite structure. The spectral bands in the range 800–900 $cm^{-1}$ containing symmetric $\nu_1$ and asymmetric $\nu_3$, P–O stretching modes of the phosphate groups were observed. The symmetric P–O stretching mode for HA occurs at 672 $cm^{-1}$. With increasing sintering temperature to 600 °C, the spectra clearly illustrate the characteristics of $\nu_4$ $PO_4$ bands at 410 and 500 $cm^{-1}$, $\nu_1$ $PO_4$ band at 670 $cm^{-1}$ and a strong, $\nu_3$ $PO_4$ absorption band in the range of 1000– 900 $cm^{-1}$ that are indicative of typical HA structure.

These spectra become stronger in intensity and better in resolution as the sintering temperature increases to 900 °C, indicating an improved molecular arrangement. At higher temperatures, IR spectra showed a considerable improvement of molecular arrangement manifested through clearly distinguishable absorption peaks. Hydroxyl stretch was observed at 2850 $cm^{-1}$ in the spectra of HA coatings before sintering. A shoulder at 432 $cm^{-1}$ between 300 and 600 °C is attributed to OH group, indicating the presence of bonded water in the film structure. However, the OH group absorption band can hardly be observed in specimens annealed at 400 °C. The characteristic peaks for $\beta$-TCP reported at 750 and 775 $cm^{-1}$ were also absent in the stoichiometric (Na /P ratio=1.49) HA coatings.

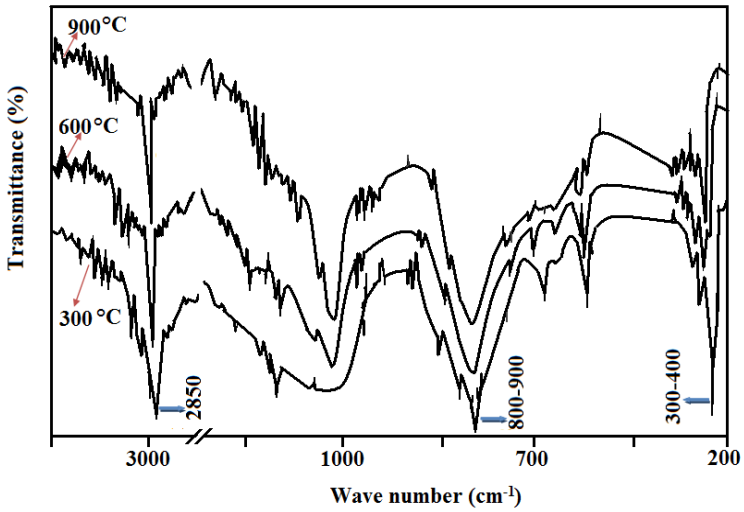


*Fig. 2. FT-IR spectrum of sol–gel derived hydroxyapatite on 316L stainless steel.*

However, in vitro tests revealed that the coating induced the formation of a semicrystalline hydroxyapatite-rich layer onto the substrate surface as a result of the chemical reaction of the biocoating with surrounding body fluid. This was considered as a preliminary signal of bioactivity after immersion in simulated body fluid solution for 40 days.

*The Pore Diameter Distribution*

Fig. 3 shows the macropore-size distribution of macroporous sol-gel glass by mercury porosimetry. The main large pore size ranges from 80 to 150 μm. The average pore diameter is 50.12 μm, and the pore volume is 0.231 mL/g. A force balance equation (Eq.1) is used to determine the sizes of pores [20]:

$$P_L - P_G = \frac{4\sigma\cos\theta}{D_P} \qquad Eq.1$$

where $P_L$ and $P_g$ are pressure of liquid and pressure of gas, respectively, σ surface tension of liquid, $\theta$ contact angle of intrusion liquid and $D_P$ pore diameter [21]. Moreover, the intrusion pressures were between 0.04 and 241 MPa in this experiment. On the other hand the average pore diameter was expressed either by length or by volume. The average pore diameter by length ($d_l$) was obtained from the following equation:

$$d_1 = 4 \times \frac{V_{tot}}{S_{tot}} \qquad Eq.2$$

where $V_{tot}$ and $S_{tot}$ are the total intruded volume of mercury and the total pore surface area, respectively. The expression is based on the assumption that the pores are cylindrical [22]. The average pore diameter by volume ($dv$) was defined as the pore diameter at which 50% of the total volume of mercury is intruded [23].

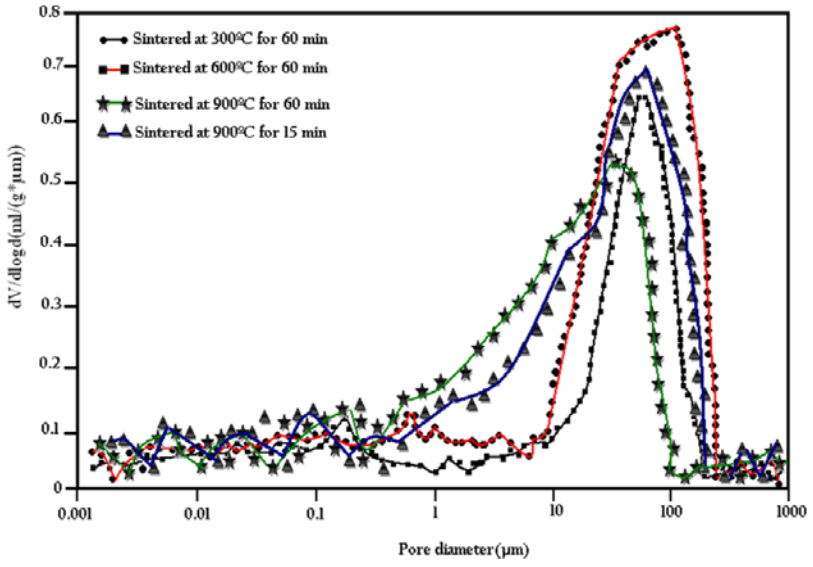


*Fig.3. Macropore-size distribution of macroporous sol-gel glass by mercury porosimetry.*

The EDX spectrum of the HA coated on 316L stainless steel surface is shown in Fig. 4, which indicates the elemental composition of the coated substrate. Intense bands of Na and P were obtained for specimens sintered at 900 °C. Small peaks corresponding to Fe, Cr and Ni present in the alloy were also detected. The intense peaks of Na and P suggest the presence of strong HA coating over the metal surface. It is concluded that by increasing the amount of $Na_2CO_3$ from 4 to 18 the presence of hydrogen was dramatically decreased.

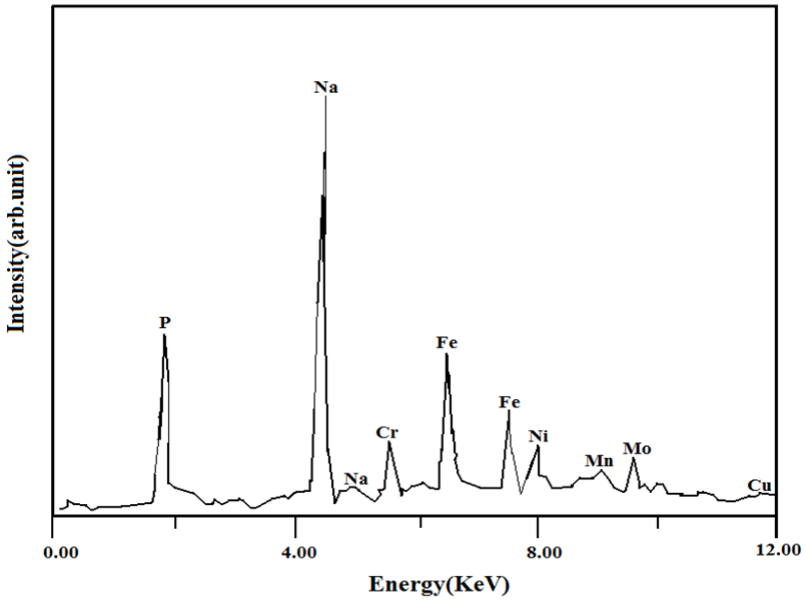


*Fig. 4. Energy dispersion X-ray analysis of HA coatings on 316L stainless steel after sintering at 900 °C.*

The EDX results indicate that the precipitated layers are composed of Na and P oxides. Their weight percentages approximately confirm the molar percentages of these oxides in prepared bioactive glass.

*Tensile Test Results*

Fig. 5 illustrates the bonding strength of the HA coatings on the 316L stainless steel substrates after sintering at different temperatures. Taking into account the average and standard deviation of the test results the interfacial bonding strength appears to be relatively constant at about 45.95MPa. The average values of bond strength are lowest at 300°C and increase with sintering temperature from 600 to 900°C. This coating strength is slightly lower than the average strength of the cured ceramic epoxy, which was determined through a blank test on sand-blasted specimens without coating to be 51.8MPa.

Mixed failure modes consisted of ceramic epoxy failure, ceramic epoxy/coating interface failure, and failure within the coating were found in all the tested specimens. However, there was not detected any coating substrate with interfacial fracture through

visual and optical microscopy examination. This indicates that the bonding at the coating/substrate interface should be stronger than the ceramic epoxy itself (Fig.6). It can be considered that the coating/substrate interfacial bonding is similar over the sintering temperatures. The presence of numerous small pores in the apatite layer at 300 °C may be one of the factors that deteriorating the mechanical integrity of the coating, resulting in a slightly decreased bonding strength.

Penetration of the ceramic epoxy glue to the substrate through the surface microcracks could have contributed to the measured bond strength. Nonetheless, because the relatively small population of the through-thickness cracks (especially at 900 °C), and because of relatively high viscosity of the ceramic epoxy glue, this contribution is expected to be negligible. The interfacial bonding between ceramic coating and metallic substrate shows improvement at the higher sintering temperatures. In general, for most coatings, the adhesive strength is a result of mechanical interlocking and chemical bonding between the coating and the underlying substrate. These results indicate that a high quality thin HA layer formed by new composition imparts biological affinity to the underlying substrates for medical uses.

A relatively good adhesion and especially excellent replication of the surface feature of the underlying substrate detected in the sol–gel dip coating of this exclusive implant material are unlikely observed in the conventional coating methods. The high strength of the sol–gel coating may be due to the intact crack free coating nature of the HA on the substrate.

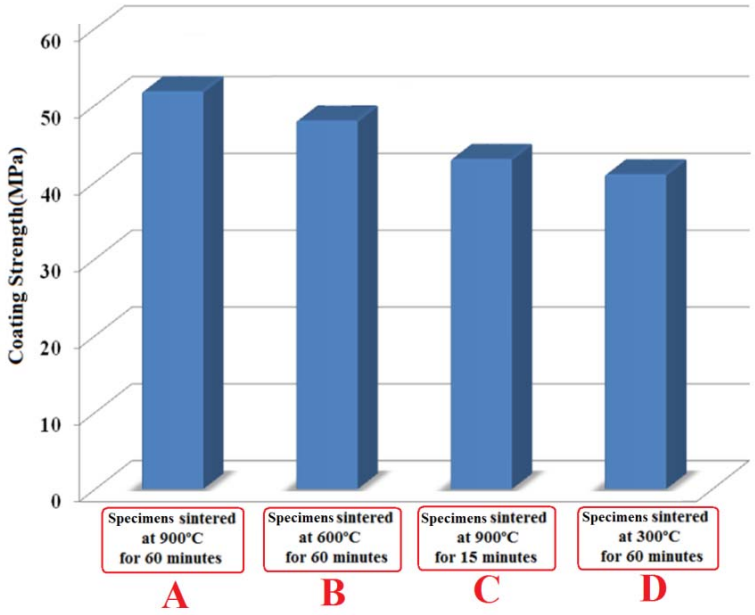


*Fig.5. The strength of the coatings prepared at different sintering temperatures.*

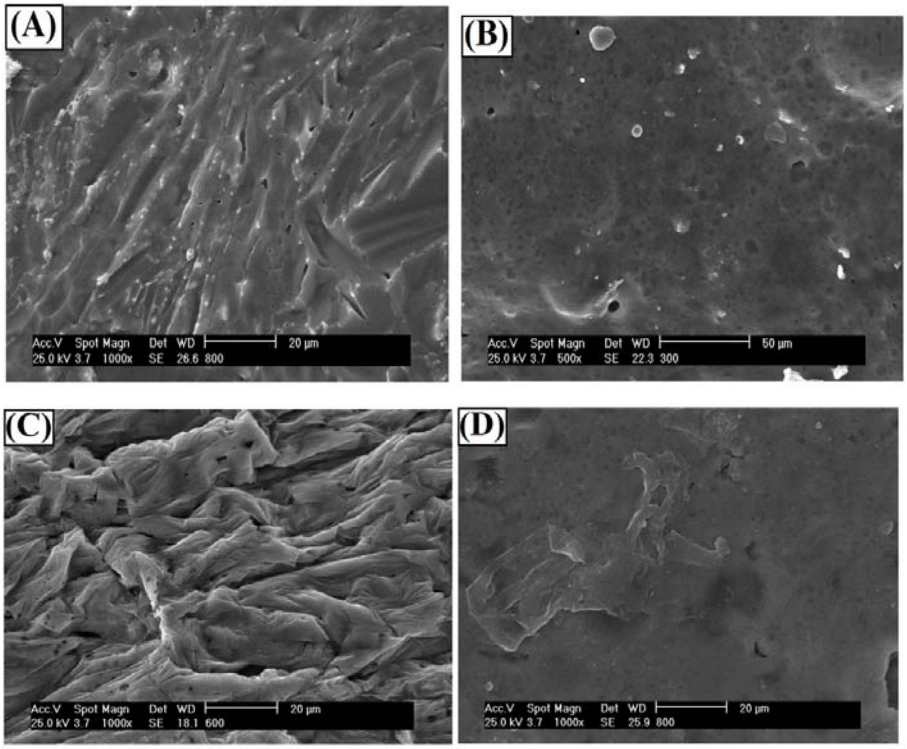


*Fig.6. Microstructure of specimens with A, B, C and D conditions shown in Fig.5.*

*Hardness Result*

For this hardness test 100g load in 20 second of indent time was used. The higher hardness values are attributed to indentation on inclined surface. The highest hardness of coated and sintered surface coating would reveal the best sintering temperature. The hardness value is increased as the sintering temperature increases. The highest hardness value achieved at 900 ºC with the value of 153 $HV_{0.1}$ which followed by 108 $HV_{0.1}$ for specimens sintered at 600ºC. The lowest harness obtained at 300 ºC with the value of only 58 $HV_{0.1}$. Consequently, it is suggested that the best sintering temperature of HA coating on stainless steel is 900 ºC (Fig. 7). The results showed that the microhardness of all specimens sintered in a vacuum furnace is slightly higher than that of specimens sintered in an argon furnace. However this difference was not quite high due to affect the general mechanical properties of the implant material.

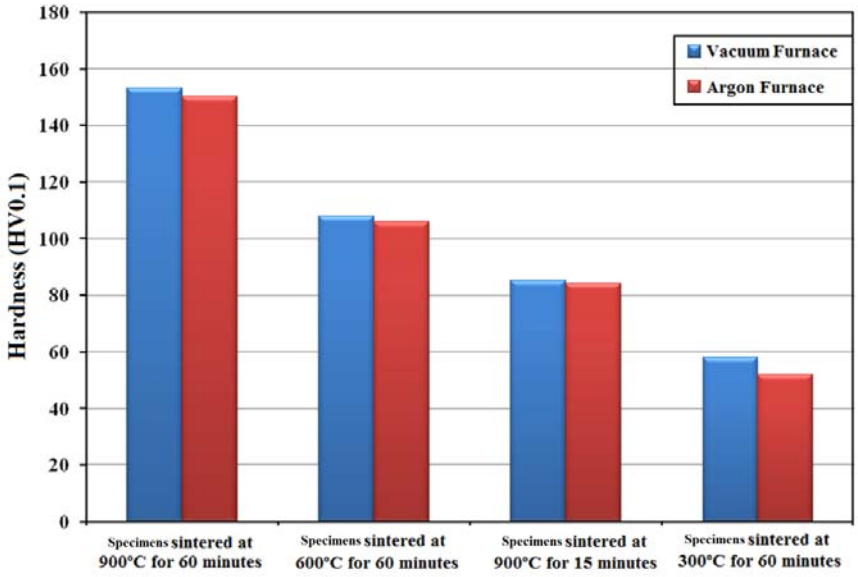


*Fig.7. The microhardness of the coatings prepared at different sintering temperatures in vacuum and argon furnace.*

*X-Ray Diffraction Analysis*

The degree of crystallinity influences dissolution of HA coating. Current study showed that the presence of higher extent of crystalline structure induced lesser dissolution of the coating. Fig. 8 (a) shows the XRD pattern of HA (Aldrich, USA) and Figs.8 (b)-(d) are showing the XRD patterns of the coating sintered at various sintering temperature. The strong reflection peak of HA powder is 31.973 of 2θ angles. The strongest peaks for HA coating sintered at 900 ºC appears in the range 29.234–31.038 of 2θ angles. As the sintering temperature increases, intensity also increases due to high crystallization rates at high temperature. The XRD results from the sintered coatings did not lead to reveal any new formation with respect to the formation of other calcium phosphate phases during sintering.

The XRD patterns indicate that the initial biocoating powder is amorphous, proving the sol–gel method could prepare pure glasses. As the sintering temperature increases up to 600 °C, some semi-sharp peaks exists in the pattern, showing that the biocoating powder still had kept the amorphous state. By further increasing of the temperature of sintering treatment, sharp peaks appear at 900 °C, indicating that crystallization occurs in the biocoating. The NaCa $(PO_3)_3$ and $Na_4KO_4$ peaks became much sharper at 900°C, corresponding to further crystallization.

XRD patterns of the gels (Fig.8 (a)-(d)) show amorphous characteristics with peaks of $NaCa(PO_3)_3$, which is an undesirable precipitate representing incomplete incorporation of calcium ions into the complex. The powders calcined at 300 °C and 600 °C exhibit two broad peaks at about 35.5° with a considerable amount of amorphous phase. With increasing calcination temperature, crystals of HA start to appear. Although it is observed that though the apatite phase started to appear at a fairly

low temperature, but complete crystallization was achieved when the powder was calcined at 900 °C.

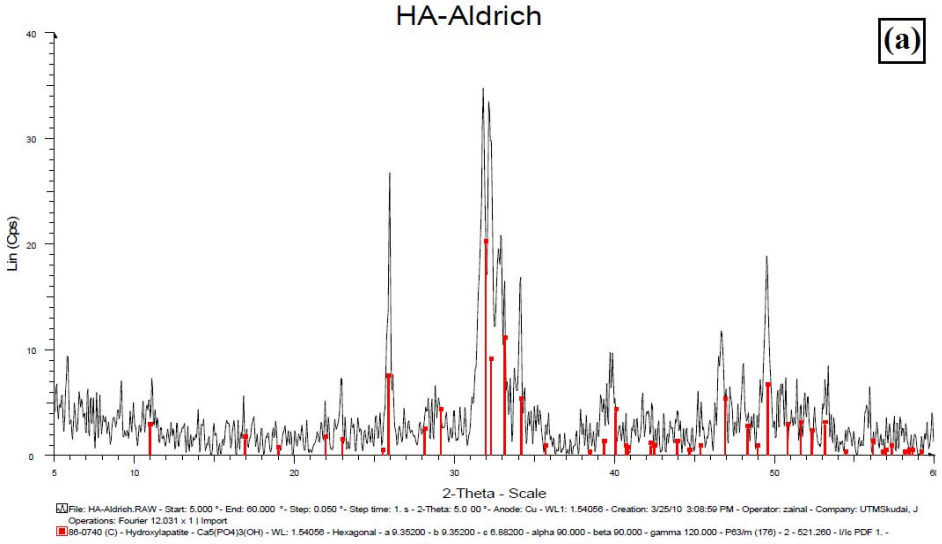


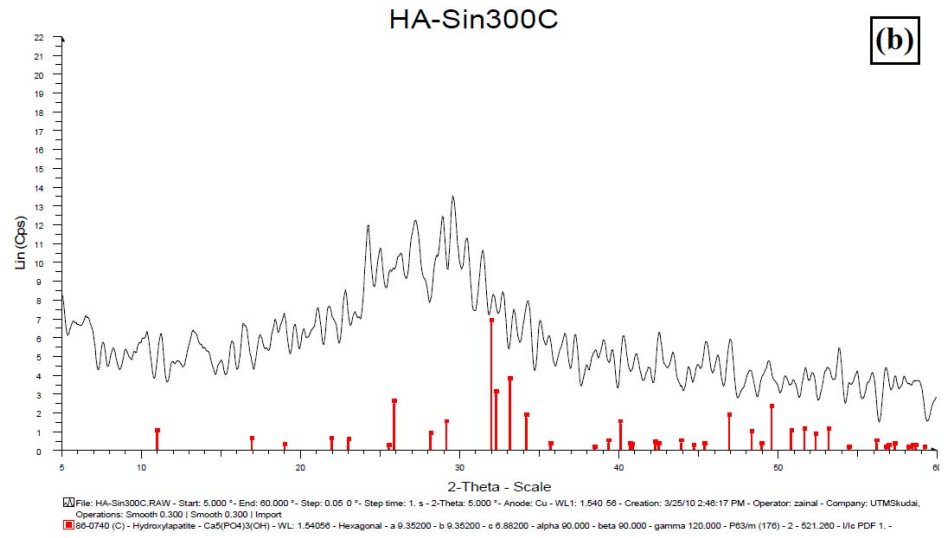

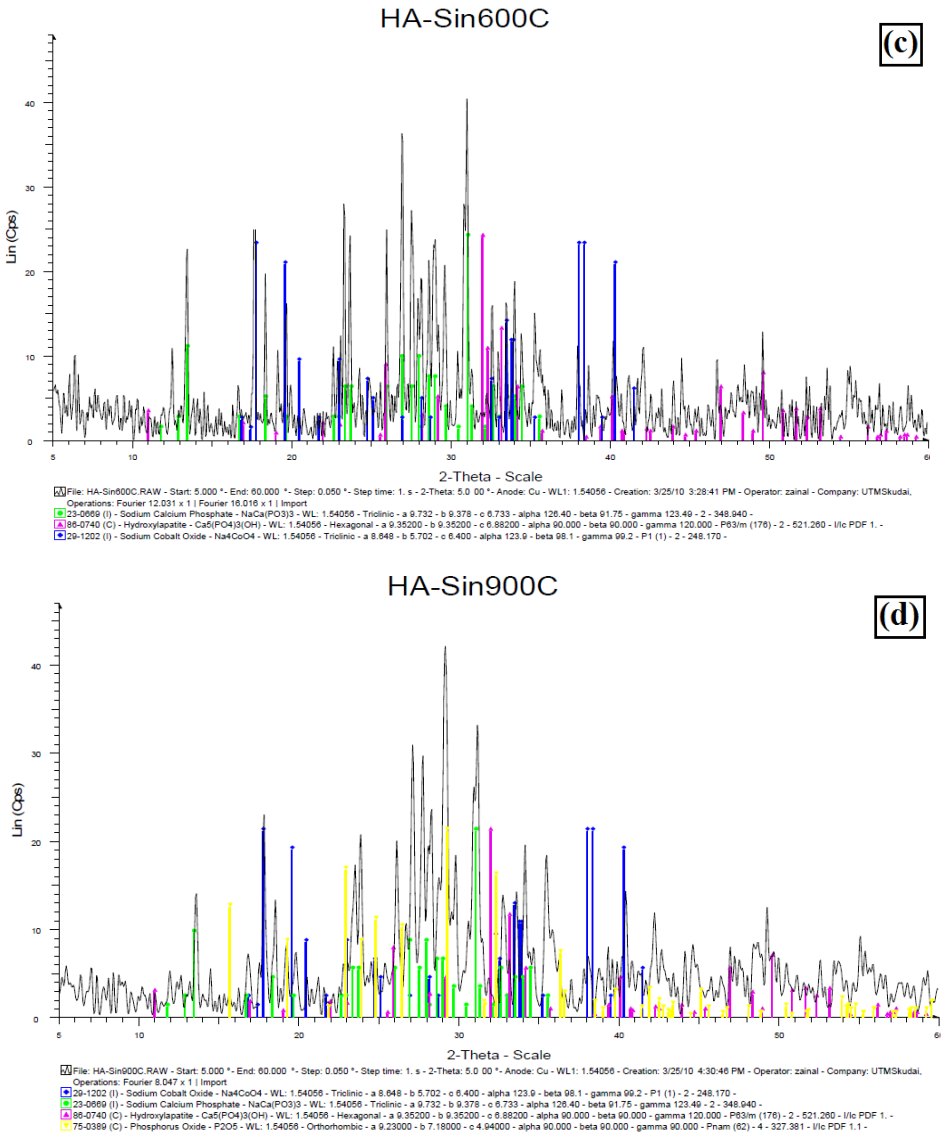


*Fig.8. XRD pattern (a) HA-Aldrich; (b) specimens sintered at 300°C; (c) specimens sintered at 600°C; (d) specimens sintered at 900°C.*

## Conclusion

Dip coating technique was applied for 316L stainless steel substrates to prepare a tight coat for orthopedic surgery applications. The sol-gel coating technique depends on the sintering temperature to obtain the desired mechanical properties. Considering the result of the FT-IR examination, hardness and tensile strength tests the most appropriate

sintering temperature is at 900°C. The particle size of the HA powder increases with the increasing of the sintering time and sintering temperature. Moreover, the microstructure of HA coating on the stainless steel is uniform at 900 °C. Besides, the porosity of the HA coating film becomes lower as the sintering temperature increases. The size of pores at 900°C of sintering temperature is less than 1.5μm. XRD pattern for HA coating shows that structural change from amorphous to crystalline occurs as the sintering temperature increases. Observation using scanning electron microscope (SEM) indicated that the coating film is uniform in terms of chemical composition and pore size at 900°C of sintering temperature.

## References

[1] D.M. Liu, Q. Yang, T. Troczynski, Journal of Biomaterial (2002), 23, pp. 691.
[2] D. Wang, G.P. Bierwagen, Progress in Organic Coatings (2009), 64, pp. 327.
[3] C. Garci, S. Cere, A. Dura□n, Journal of Non-Crystalline Solids (2004), 348, pp. 218.
[4] R.B. Heimann , et al., J Mater Sci Mater Med. 2008 Oct;19(10):pp. 295.
[5] M. Akao, H. Aoki, K. Kato, J. Mater. Sci., 16(1981), pp. 809.
[6] J. Romian, S. Padilla, M. Vallet, Chem. Mater., 15(2003), No.4, pp. 798.
[7] P. Sepulveda, J.R. Jones, and L.L. Hench, J. Biomed. Mater. Res., 61(2002), No.2, pp. 301.
[8] L. Fu, K.A. Khor, J.P. Lim, Materials Science and Engineering A, Volume 316, Issues 1-2, 15 November 2001, pp.46.
[9] J.R. Woodard, et al., Biomaterials Volume 28, Issue 1, January 2007, pp. 45.
[10] L.E. Amato, D.A. Lo´pez, P.G. Galliano, S.M. Cere´, Mater. Lett. 59 (2005), pp. 56.
[11] O. Peitl, E.D. Zanotto, L.L. Hench, J. Non-Cryst. Solids 292 (2001), pp. 115–126.
[12] L. Fu, K.A. Khor, J.P. Lim, Surface and Coatings Technology, 127(2000), pp. 66-75.
[13] C. Garcia, S. Cere, A. Duran, Non-Cryst. Solids, 348 (2004), pp. 218–224.
[14] C. Garcı´a, S. Cere´, A. Dura´n, J. Non-Cryst. Solids, 352 (32–35) (2006), pp. 3488.
[15] K.A. Gross, C.S. Chai, G.S.K. Kannangara, B. Bin-Nissan, L. Hanley, J Mater Sci Mater Med 1998; 9:839-43.
[16] C.S. Chai, K.A. Gross, B. Ben-Nissan, Biomaterials, 1998, 19:2291-6.
[17] H. Takahashi, et al., Eur J Solid State Inorg Chem, 1995, 32:829-35.
[18] Q. Qiu, P. Vincent, B. Lowenberg, M. Sayer, J.E. Davies, Cells Mater 1993, 3(4):351-60.
[19] A.C. Chapman, L.E. Thirlwell, Spectrochim, Acta, 20 (1964) 937.
[20] C. Salmas and G. Androutsopoulos, Journal of Colloid and Interface Science, Vol. 239, Issue 1, 1 July 2001, pp. 178-189.
[21] R.P. Mayer and R.A. Stowe, Journal of Colloid Science Vol. 20, Issue 8, October 1965, pp. 893-911
[22] L.C. Drake and H.L. Ritter, Ind. Eng. Chem. 17 (1945), pp. 787–791
[23] P.J. Dees and J. Polderman, Powder Technol. 29 (1981), pp. 187–197.